

THE INTERNATIONAL RESEARCH GROUP ON WOOD PROTECTION

**Guidelines for the preparation of a full scientific paper for an IRG
Scientific Conference**

NB

Please note that papers received after the deadline 1 March 2020 will be posted on the website (Compendium) but the opportunity to make an oral presentation will be at the discretion of the Scientific Programme Committee chair. These papers may be presented as posters at the meeting. Deadline for submitting extended abstract or short papers for poster presentations is 1 April 2020.

**IRG SECRETARIAT
Box 5604
SE-114 86 Stockholm
Sweden
www.irg-wp.com**

Dear author of the IRG paper!

Allocation of the papers to different sections is one of the most challenging tasks for the Scientific Programme Committee (SPC). In order to prepare good programme for the upcoming conference, we would like to ask you for assistance. Please tick, the most appropriate Working Party, where your paper fits most. SPC will try to consider your opinion.

Section 1. Biology	WP 1.1. Soft rot, bacteria, bluestain and moulds	<input type="checkbox"/>
	WP 1.2. Basidiomycetes	<input type="checkbox"/>
	WP 1.3. Insect biology and testing	<input type="checkbox"/>
	WP 1.4. Natural durability	<input type="checkbox"/>
	WP 1.5. Marine	<input type="checkbox"/>
	WP 1.6. Cultural Artefact Protection	<input type="checkbox"/>
Section 2. Test Methodology and Assessment	WP 2.1. Prediction of service life	<input type="checkbox"/>
	WP 2.2. Microbial test methodology	<input type="checkbox"/>
	WP 2.3. Chemical/physical analysis	<input type="checkbox"/>
	WP 2.4. International Standardisation	<input type="checkbox"/>
Section 3. Wood Protecting Chemicals	WP 3.1. Inorganic preservatives	<input type="checkbox"/>
	WP 3.2. Organic preservatives	<input type="checkbox"/>
	WP 3.3. Performance - lab & field tests	<input type="checkbox"/>
	WP 3.4. Fire retardants	<input type="checkbox"/>
Section 4. Processes and Properties	WP 4.1. Chemical wood modification	<input type="checkbox"/>
	WP 4.2. Wood composites, WPCs and Engineered wood products	<input type="checkbox"/>
	WP 4.3. Treating processes & treatability of timber	<input type="checkbox"/>
	WP 4.4. Coatings, hydrophobic treatments and surface aspects	<input checked="" type="checkbox"/>
	WP 4.5. Thermal wood modification	<input type="checkbox"/>
	WP 4.6. Fire protection	<input type="checkbox"/>
	WP 4.7. Protection by design	<input type="checkbox"/>
Section 5. Sustainability and Environment	WP 5.1. Environment	<input type="checkbox"/>
	WP 5.2. Sustainability	<input type="checkbox"/>

This paper is intended for the special session on:

- Protection Against Wood Borers in the Marine Environment
 Surface Treatments and Characterization

This paper will be presented as a(n):

- Oral presentation (15 minutes + questions)

Poster presentation (including a 3-minute oral presentation)

This paper will most probably be presented by: Sebastian Dahle

sebastian.dahle@bf.uni-lj.si

This paper may be listed as part of the Proceedings according to the Clarivate index system.

THE INTERNATIONAL RESEARCH GROUP ON WOOD PROTECTION

Special session

Surface Treatments and Characterization

Performance of a water-borne stain on beech, spruce, MDF and OSB improved by plasma pre-treatment

Sebastian Dahle, Jure Žigon, Marko Petrič
University of Ljubljana, Biotechnical Faculty
Department of Wood Science and Technology
Jamnikarjeva ulica 101
1000 Ljubljana, Slovenia

Irena Uranjek
Rogač Plus d.o.o.
Mariborska cesta 103
2312 Orehova vas, Slovenia

Paper prepared for the IRG51 Scientific Conference on Wood Protection
Bled, Slovenia
8-11 June 2020

Disclaimer

The opinions expressed in this document are those of the author(s) and are not necessarily the opinions or policy of the IRG Organization.

IRG SECRETARIAT
Box 5604
SE-114 86 Stockholm
Sweden
www.irg-wp.com

Performance of a water-borne stain on beech, spruce, MDF and OSB improved by plasma pre-treatment

Sebastian Dahle¹, Jure Žigon², Irena Uranjek³, Marko Petrič⁴

¹ University of Ljubljana, Biotechnical Faculty, Department of Wood Science and Technology, Ljubljana, Slovenia (UL BF), Assistant professor, Postdoc, sebastian.dahle@bf.uni-lj.si

² (UL BF), Technical adviser and PhD candidate, jure.zigon@bf.uni-lj.si

³ Rogáč Plus d.o.o., Mariborska cesta 103, 2312 Orehova vas, Slovenia, irena@rogacplus.si

⁴ (UL BF), Full professor, marko.petric@bf.uni-lj.si

ABSTRACT

The performance of protective wood coatings, especially under outdoor weathering, depends on many factors, including the interface between coating and substrate. Sufficient interactions are particularly difficult to achieve on several types of wood-based composites, such as oriented strand boards (OSB) and medium-dense fibreboards (MDF). The interface between wood-based substrates and coatings can be modified and optimized by different means, e.g. by sanding or by using appropriate chemical primers. Plasma treatments represent a very interesting technique for surface modification, as they do not require additional reactants or chemicals, and therefore are an environmentally friendly alternative for optimizing the interface.

The studies were performed on Norway spruce (*Picea abies* (L.) Karst.) and common beech (*Fagus sylvatica* L.) wood, OSB and MDF using a commercial waterborne stain for exterior application and a commercial plasma unit (PlasmaTreat OpenAir®). Artificial accelerated weathering (AAW), water immersion and adhesion strength testing were conducted to test the performances of the surface systems formed by coating and surface, whereas their morphology and appearance was evaluated using confocal laser scanning microscopy (CLSM), gloss, and colour CIELAB system.

On coated solid spruce wood, the plasma pre-treatments yielded a slight reduction of the colour change during AAW and remaining gloss after AAW at approx. doubled values as compared to non-treated specimen. The initial bond strength of the coating of approx. 4 MPa was well preserved after AAW on plasma pre-treated samples, but reduced by 13 % on the non-treated specimens.

On coated beech wood, the colour change of the stain during AAW increased on plasma pre-treated specimen, whereas gloss, morphology, and bond strength were not influenced by the plasma pre-treatments.

On coated MDF specimen, the plasma pre-treatments yielded again a slight reduction of the colour change during AAW and a remaining gloss after AAW at approx. doubled values as compared to non-treated specimen. The weathering led to the formation of valleys and ridges on the surface of the non-treated specimens, but not on the plasma pre-treated ones. Further, the thickness swelling of the non-treated MDF specimen was larger by 12.7 % as compared to the thickness swelling of the plasma pre-treated specimen. The coating's adhesion strength on MDF was solely defined by the substrate material and did not show any differences due to plasma pre-treatments.

On surface finished OSB, the colour change of the stain during AAW was slightly lower on plasma pre-treated specimen, but gloss and morphology were comparable in all cases.

Keywords: Coating, weathering, plasma, wood, composite

1 INTRODUCTION

The application of wooden and of wood-based materials in many cases requires protection or an improved inherent resistance against physical and chemical influences. This is especially required for outside applications, where natural weathering causes fast deterioration of the material. A suitable protection can be obtained through coating systems, but the performance strongly depends on the selected coating and the type of substrate (Keskin and Tekin 2011; Veigel *et al.* 2014). In particular, the performance of the protective coating is influenced by the chemical properties and anatomical structure of the substrate material, as well as by its density and surface roughness. Furthermore, the performance of the entire surface system depends on the compatibility between the substrate material and the selected coating (Nemli and Hiziroglu 2009; Istek *et al.* 2010; Rolleri and Roffael 2010; Bardak *et al.* 2011).

Surface systems pose particular problems for different kinds of wood-plastic composites, as environmental friendly formulations of surface systems and water-borne coatings can hardly meet the requirements of such composites. Few water-borne coatings for these composite materials are under investigation, like an acrylic coating that Durmaz and co-workers (2020) used on wood-plastic composite (WPC) materials for exterior applications. A crucial factor for the performance of WPC products in general, and in particular for oriented strand board (OSB) and medium density fibreboard (MDF), is the moisture ingress into the bulk leading to the degradation of the material. This is a sincere challenge for most protective coatings, but can be counteracted e.g. by elaborate organosilicon systems (De Vetter *et al.* 2011) or thermal spray coatings (Nejad *et al.* 2017). A further important effect of weathering is the decolouration of the material (Kiguchi *et al.* 2007).

Good means to modify the interface between wood-based materials and coatings are provided by plasma treatments of the substrate (Žigon *et al.* 2018; Altgen *et al.* 2019). The effects of plasma treatments on the treated surfaces are induced through physical and chemical processes at the work pieces' surfaces (Wolkenhauer *et al.* 2008, Altgen *et al.* 2015). These processes modify the surface free energy (Blanchard *et al.* 2009), can etch the surfaces (Jamali and Evans 2011) or activate the surface (Žigon *et al.* 2019). Through these modifications, enhancements are achieved regarding penetration, adhesion of the applied polymer and final properties of the formed surface system (Dam 2017; Liston *et al.* 1993; Wolkenhauer *et al.* 2009; Wolf and Sparavigna 2010; De Cademartori *et al.* 2016; Perisse *et al.* 2017; Reinprecht *et al.* 2018). Especially an improved adhesion was reported multiple times for different plasma treatments, for various coating or glue systems, and for diverse wooden and wood-based substrates (Riedl *et al.* 2014; De Cademartori *et al.* 2016; Lütke-meier *et al.* 2016; Wascher *et al.* 2017). In some cases, this has led to improved durability of coatings (Podgorski and Roux 1999). Further groups found enhanced resistance to weathering (Haase *et al.* 2019) or water exposure, which is correlated with an enhancement of the interface as well as modified bulk properties near the wood material's surface (Wascher *et al.* 2014; Haase *et al.* 2019).

The plasma technology that has been used on wooden and wood-based substrates mostly employs dielectric barrier discharges (DBD). A majority of these utilize air as operating gas for the plasma treatments (Žigon *et al.* 2018). The reason for this is, that DBD air plasmas are a simple, cost efficient, and clean technology to improve coating and adhesive bond performance on various substrates. However, such direct DBD plasma treatments are limited in the thickness of samples that can be treated; therefore, many applications focus on veneers, chips, particles, fibres, or powder. Although there are approaches to overcome this limitation (c.f. Žigon *et al.* 2018; Žigon and Dahle 2019), the most versatile techniques are remote plasma treatments, so-called plasma jets, as those are applicable to a wide variety of substrates with different thicknesses, chemical composition, geometrical shapes and other properties.

However, the use of plasma jet systems was hitherto restricted to few high-value applications. In 2014, Melamies found a sixfold improved wax adsorption on racing skis after using a commercial gliding arc plasma pre-treatment. According to Jordá-Vilaplana and co-workers (2015), the bond strength in polylactic acid (PLA) joints with bio-based adhesives was strongly improved through similar plasma treatments, indicating it's worth e.g. in correlation with 3D-printed parts, which oftentimes use PLA as base material. At LIGNA (2013), the cleaning of up to 3 m wide WPC boards was presented together with an improved finishing of board sides using edge bands at lower costs and energy uptake as compared to currently used laser processes. Hämäläinen and Kärki (2013) treated WPCs from polypropylene and spruce wood, using another commercial gliding arc plasma system. Thereby they yielded an improved adhesion after bonding specimens with PVAc glue. Kraus and co-workers (2015) conducted a wide comparison on WPC gluing and possible means to improve the performance of the joints. Out of a variety of methods, Kraus found the most determining factors for the selection of the best-suited method to be the matrix material of the WPC and the surface free energy of the work piece. They also pointed out the possibility of overtreatments, which led to a significant reduction of the mechanical performance. Amongst all different methods, low-pressure plasmas provided the highest reproducibility, whereas atmospheric pressure plasmas possess a much higher mobility. Although localized, these methods are available and easy to use particularly for large-area and three dimensionally shaped work pieces (Straccia *et al.* 2008). Baltazar-Y-Jimenez and Bismarck (2007) used a similar plasma system to modify lignocellulosic fibres, influencing their surface chemistry, surface free energy, and pH-dependent zeta potential. For the use in WPC applications, the positive impact of an improved adhesion is accompanied with a deterioration of the fibres mechanical properties due to heat and etching from the plasma (Baltazar-Y-Jimenez *et al.* 2008), thus giving another indication on the importance of optimization for any plasma treatment on organic and natural materials.

In this study, we use a gliding arc jet as a commercial plasma technique that overcomes many of the limitations of other plasma systems, which have been used previously on wooden and wood-based substrates. The influence of this plasma technique on the performance of different classes of wood-based materials is investigated exemplarily with a water-based coating system for outdoor applications. As the substrates, solid spruce, solid beech, an MDF and an OSB boards were chosen, which represent the most common softwood and hardwood species as well as two of the most common composite materials, respectively. With regards to the application, appearance and performance were studied before and after accelerated artificial weathering in terms of colour change, gloss, coating adhesion strength, and liquid water permeability.

2 EXPERIMENTAL METHODS

All data is made available via Zenodo (Dahle *et al.* 2020).

2.1 Sample preparation and application of coating

The common beech and Norway spruce planks with semi-radial orientation of wood fibres were collected from raw material without any defects, while OSB and MDF were gained by local supplier in Slovenia. From each material, samples with dimensions of $(300 \times 75 \times 19) \text{ mm}^3$ (length \times width \times thickness) were prepared. All samples were conditioned in a room with a temperature of 20 °C and relative humidity of 65 % to reach equilibrium moisture content before coating application. A pigmented waterborne acrylic stain (Belinka Exterior, Belinka Belles, d.o.o., Ljubljana, Slovenia) was applied manually on control and plasma pre-treated (explained in next section) with a quadruple coating applicator, at the rate of movement of approximately 30 mm/s. The wet film thickness of the coating layer was 240 μm . The coated samples were stored in a dark room for 21 days before future experimental work.

2.2 Plasma treatments

Plasma treatments (PT) were carried out using an Openair® unit (PlasmaTreat GmbH, Steinhagen, Germany) with a RD1004 head rotating at 2800 min^{-1} and base modules FG5001, HTR12, and DVE10. Electric parameters during plasma treatments were device's parameters $U = 280 \text{ V}$, $I = 15.6 \text{ A}$, $PP = 21.0 \text{ kHz}$, and $PLT = 100\%$. Pressurized air was supplied at 4 bar.

PT were optimized for each substrate according to the apparent water contact angles (WCA) as determined using a Surface Analyst 2001 (BTG Labs, St. Bernard, OH, USA).

2.2.1 Optimization of PT on MDF

The untreated MDF substrates exhibited an average WCA of 94° . Out of a series of tests with different working distances, speeds, and nozzle types as presented in Table 1, the following treatment parameters were selected:

- Plasma treatment PT A: PTF2647-1, $d = 4 \text{ mm}$, $v = 10 \text{ m}\cdot\text{min}^{-1}$, scan width $\Delta = 20 \text{ mm}$, 1 pass
- Plasma treatment PT B: PTF774-1, $d = 4 \text{ mm}$, $v = 6 \text{ m/min}$, scan width $\Delta = 45 \text{ mm}$, 2 passes

Table 1: Parameter study on water contact angles to optimize plasma treatments on MDF using single pass (1× PT) and double pass plasma treatments (2× PT) depending on working distance, substrate feed speed and plasma nozzle.

Working distance d [mm]	Speed v [$\text{m}\cdot\text{min}^{-1}$]	Nozzle type with (die opening)	1× PT	2× PT
6	6	PTF2647-1 (14°)	40°	28°
	4	PTF2647-1 (14°)	48°	–
		PTF958-1 (5°)	9°	–
4	6	PTF774-1 (25°)	44°	32°
		PTF570-1 (32°)	65°	52°
	10	PTF2647-1 (14°)	30°	62°

2.2.2 Optimization of PT on solid beech and spruce

The untreated substrates exhibited an average WCA of 52° for beech and 40° for spruce. Out of a series of tests with different working distances, speeds, and nozzles as presented in Table 2, the following treatment parameters were selected:

- Plasma treatment PT C: PTF570-1, $d = 4 \text{ mm}$, $v = 10 \text{ m/min}$, $\Delta = 50 \text{ mm}$, 1x pass
- Plasma treatment PT D: PTF570-1, $d = 4 \text{ mm}$, $v = 20 \text{ m/min}$, $\Delta = 50 \text{ mm}$, 1x pass

Table 2: Parameter study on water contact angles to optimize PT on beech and spruce using single pass (1x PT) and double pass plasma treatments (2x PT) depending on working distance, substrate feed speed and plasma nozzle.

Working distance d [mm]	Speed v [$\text{m}\cdot\text{min}^{-1}$]	Nozzle type with (die opening)	1× PT	2× PT
4	6	PTF774-1 (25°)	26°	9°
		PTF570-1 (32°)	28°	21°
	10	PTF570-1 (32°)	5°	7°
	20	PTF570-1 (32°)	21°	20°

2.2.3 Optimization of plasma treatments on OSB

The untreated OSB substrates exhibited an average WCA of 99°. Due to the paraffin finish commonly applied to OSB products, cleaning the surface with isopropanol (IP) before plasma treatments was tested. IP cleaning reduced the WCA down to 41°, but combinations of IP cleaning and subsequent PT yielded the same contact angles that plasma treatments without IP pre-cleaning did. Therefore, no IP cleaning was included in the main part of this study. Due to strong inhomogeneity and roughness of the OSB surface, only one set of parameters was selected, but twice as much specimen were prepared as for MDF and solid wood. Out of a series of tests with different working distances, speeds, and nozzles as presented in Table 3, the following treatment parameters were selected:

- Plasma treatment E: PTF2647-1, $d = 4$ mm, $v = 4$ m/min, $\Delta = 20$ mm, 1x pass

Table 3: Parameter study on water contact angles to optimize plasma treatments on OSB using single pass (1x PT) and double pass plasma treatments (2x PT) depending on working distance, substrate feed speed and plasma nozzle.

Working distance d [mm]	Speed v [m·min ⁻¹]	Nozzle type with (die opening)	1× PT	2× PT
4	10	PTF570-1 (32°)	97°	–
	6	PTF2647-1 (14°)	38°	39°
	4	PTF2647-1 (14°)	36°, 27°, 31°	35°
		PTF958-1 (5°)	Burning traces	–
	10	PTF958-1 (5°)	65°	–
6		PTF958-1 (5°)	45°	–

2.3 Artificial accelerated weathering

Artificial accelerated weathering (AAW) was conducted using an Atlas SUNTEST XXL+ chamber (Atlas Material Testing Technology, Mount Prospect, IL, USA) according to the method 1A for exterior applications described in EN ISO 11341 (2004). The parameters and conditions during the AAW test were as follows: irradiance at 340 nm set to an irradiation power of 0.35 W·m⁻², relative humidity of 65 %, chamber temperature of 35 °C and the temperature on the black panel sensor of 55 °C. AAW was interrupted for gloss and colour measurements after 10 hours and 50 hours of aging. After a total aging time of 63 hours, the AAW process was terminated.

2.4 Colour and gloss measurements

Colour measurements were performed using an X-Rite (Grand Rapids, MI, USA) SP62 spectrophotometer using a D65-type light source. On all samples, three reproducible spots in the front, back and centre of the samples were selected for measurements before, during and after weathering (c.f. section 2.3). The CIELAB parameters (L^* , a^* , and b^*), their changes (ΔL^* , Δa^* , and Δb^*), and the total colour change (ΔE^*) were determined after the CIEDE2000 formula (CIE 2000), using the MS Excel template provided by Sharma *et al.* (2020) in accordance with Sharma *et al.* (2005). These values were then arithmetically averaged for each sample.

The gloss values were determined in accordance with EN ISO 2813 (1997) under incident light angles of 20°, 60°, and 85° using an X-Rite (USA) AcuGloss TRI instrument. On all samples, two reproducible spots in the front and back were selected for measurements before, during and after weathering. The determined values were then arithmetically averaged for each sample.

2.5 Confocal laser scanning microscopy

The surface morphology of the different samples was investigated using a confocal laser scanning microscope (CLSM) LEXT OLS5000 (Olympus, Tokyo, Japan) equipped with a laser light source

with a wavelength of 405 nm. Height differences and root mean square (RMS) roughness (Sq) were evaluated through the equipment's software (OLS50-S-AA, Olympus, Tokyo, Japan).

2.6 Adhesion strength testing

The adhesion of the coatings was tested on both, plasma treated and reference specimens, using pull-off test 4 weeks after the application of the coatings following the standard EN ISO 4246 (2016). Aluminium dollies with a diameter of 20 mm were glued onto the coated wood surface using a two-component epoxy resin and cured for 24 h. The coating directly surrounding the glued dollies was carefully cut off down to the substrate to avoid propagation of failures out of the tested area. The adhesion strengths were determined using a pull-off testing machine (DeFelsko, Ogdensburg, USA) until the dolly separated from the specimen. If a separation occurs between the substrate and the coating in at least 60 % of the tests area, the resulting pull-off strength is considered an adhesive one, otherwise a cohesive one.

2.7 Liquid water permeability

Assessment of the liquid water permeability was determined according to modified standard EN ISO 927-5 (2007). Specimens with dimensions of $(100 \times 75 \times 19) \text{ mm}^3$ were cut from both, plasma pre-treated and reference specimens of each material. Except on the side with applied coating, the specimens were sealed with 2-component epoxide coating Epolor HB (Color, Medvode, Slovenia). The specimens were not preconditioned before actual testing. After the sealing coating was cured, the samples were placed on the surface of water in a batch for 72 h. The increment of samples mass gained during permeability test was calculated (in $\text{g}\cdot\text{m}^{-2}$).

3 RESULTS AND DISCUSSION

3.1 Performance of coated MDF samples

The colour change during the AAW is much less pronounced on coated MDF, if a plasma pre-treatment was carried out prior to the coating application. The colour changes in a^* and b^* values are comparable on the plasma pre-treated sample and also on the reference sample. The detailed values are summarized in Table 4.

Table 4: Change of CIELAB colour parameters with increasing time of AAW time on plasma pre-treated (PTA) and non-treated (NT) coated MDF samples.

Weathering time / h	NT				PTA			
	ΔE	ΔL^*	Δa^*	Δb^*	ΔE	ΔL^*	Δa^*	Δb^*
10	3.36	-2.04	-2.39	-3.60	1.84	-0.42	-1.42	-1.79
50	7.69	-4.22	-6.01	-6.91	5.00	-1.62	-4.06	-3.65
63	6.68	-3.73	-5.14	-6.32	4.29	-1.32	-3.46	-3.34

Figure 1 shows the development of the gloss values under 20° , 60° and 85° incident light angle for both, the plasma pre-treated and the non-treated reference samples. After weathering, the gloss is strongly reduced and with the remaining gloss being higher on the plasma pre-treated samples by a factor of 1.4 and 2.1 at 60° and 85° , respectively. The detailed values are summarized in Table S1 (Dahle et al. 2020).

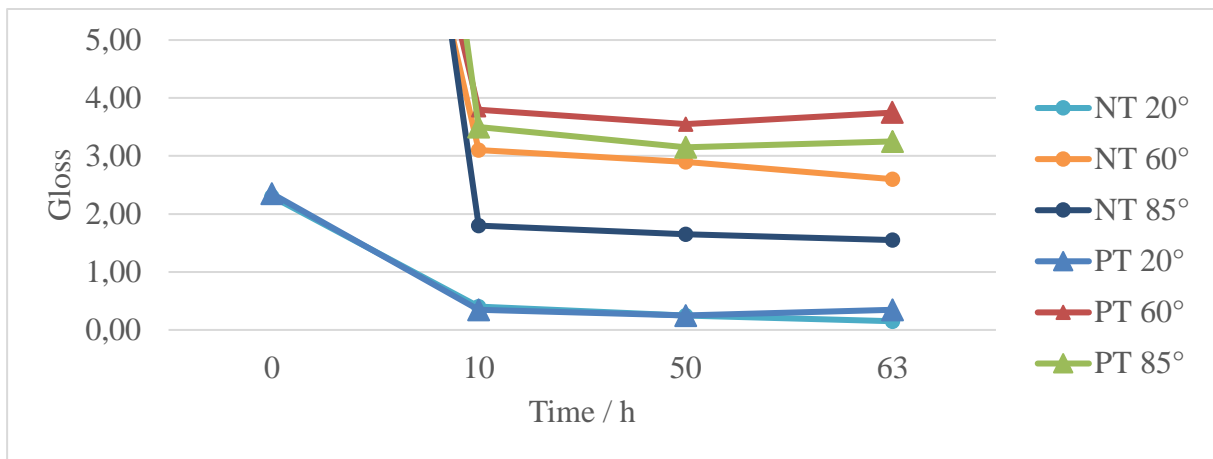


Figure 1: Change of gloss value under 20°, 60° and 85° over AAW time on plasma pre-treated (PTA) and non-treated (NT) coated MDF samples

After AAW for 63 h in outdoor conditions, the non-treated, coated MDF reference specimen exhibited a thickness of 31.5 mm, corresponding to a height increase of 66 %, whereas the plasma pre-treated, coated MDF specimen's thickness amounted to 30.1 mm, corresponding to a height increase of 58.4 %. During the test, the back and the sides of both samples were uncovered, thus providing large open areas for the uptake of water from the wet weathering cycles. The plasma pre-treatment and its increase of the coating's performance still did reduce the overall swelling by a relative factor of $0.584 / 0.658 = 0.888$.

Figure 2 depicts CLSM images of a non-treated, coated MDF specimen after 63 h of AAW. The left image shows an area at 20× magnification, corresponding to a total depicted area of $(643 \times 644) \mu\text{m}^2$, in which the vertical range amounts to $\Delta Z = 228 \mu\text{m}$. The right image shows an area at 50× magnification, corresponding to dimensions of $(256 \times 257) \mu\text{m}^2$, in which the vertical range is $\Delta Z = 67 \mu\text{m}$.

In comparison, Figure 3 displays corresponding CLSM images of a plasma pre-treated (PTA), coated MDF specimen after 63 h of AAW at 20× (left) and 50× magnification (right) with vertical ranges of $\Delta Z = 172 \mu\text{m}$ and $\Delta Z = 65 \mu\text{m}$, respectively.

The surface of the non-treated reference sample is highly uneven as strongly pronounced valleys and ridges have formed during AAW, which is reflected in a roughness value of $Sq = 19.8 \mu\text{m}$. In comparison, the plasma-treated sample does not develop similar structures during weathering, which is represented by a much lower roughness value of $Sq = 8.7 \mu\text{m}$. At higher magnification, both samples show comparable surface structures with regularly distributed particles (diameters $\sim 10 \mu\text{m}$) and few small dips. At 50× magnification, the roughness of the non-treated sample of $Sq = 5.8 \mu\text{m}$ is still higher compared to a roughness of $Sq = 2.8 \mu\text{m}$ for the plasma-treated sample; however, this seems to be due to the remaining slopes on the surface rather than the microstructures.

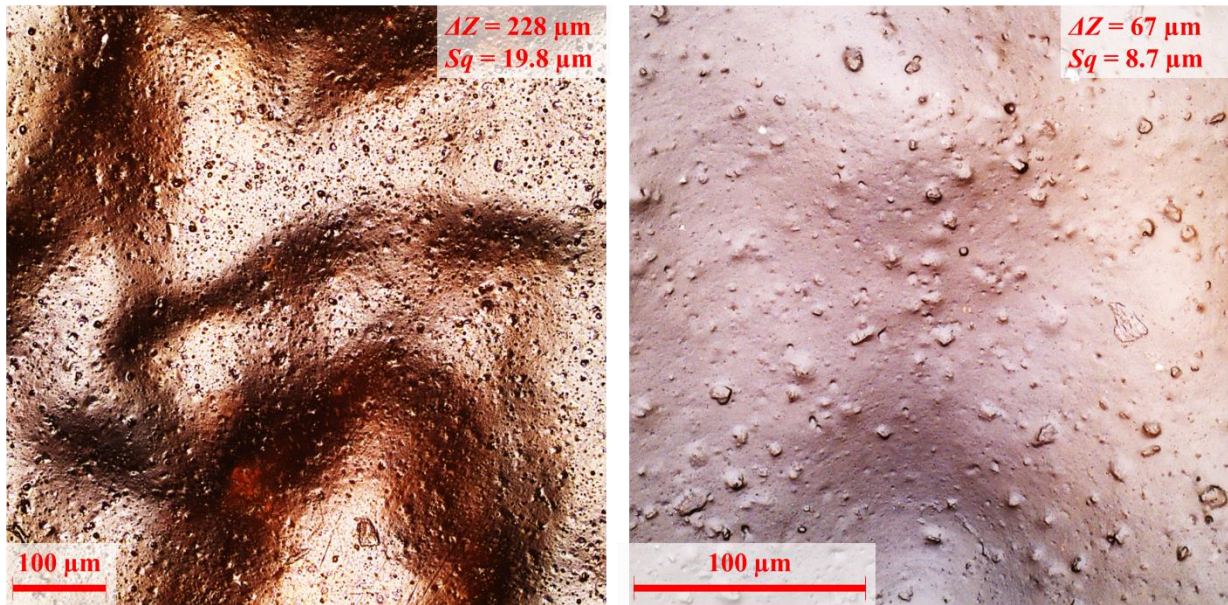


Figure 2: CLSM images of the coated MDF reference sample after 63 h of weathering at 20× (left) and 50× magnification (right).

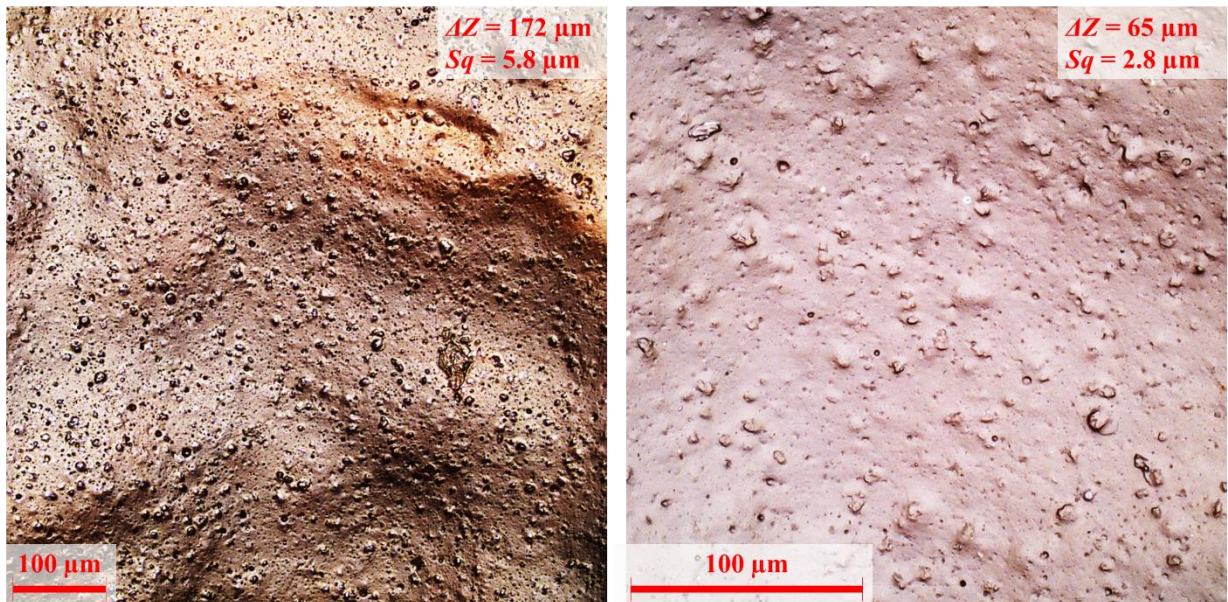


Figure 3: CLSM images of the plasma pre-treated (PTA), coated MDF sample after 63 h of weathering at 20× (left) and 50× magnification (right).

Figure 4 exhibits the results for adhesion strengths and the corresponding standard deviations from series of pull-off tests on both, the coated reference (NT) and the MDF specimens treated according to protocols plasma treatment A (PTA) and plasma treatment B (PTB) as described in section 2.2.1. The tests were carried out both, on as-prepared samples and on samples after 63 h of AAW. The MDF samples after AAW, however, exhibited such weak mechanical properties of the aged MDF bulk material, that all tests yielded a cohesive failure inside the substrates. As-prepared specimen yielded adhesion strengths slightly above 2 MPa and did not show any significant difference between non-treated and two plasma-treated specimen (PTA, PTB).

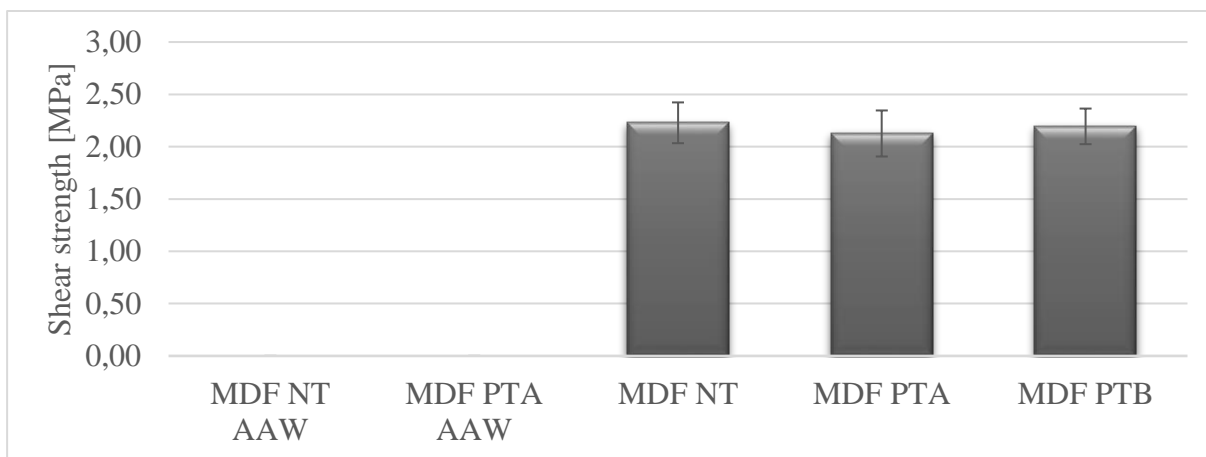


Figure 4: Adhesion strengths and corresponding standard deviations from pull-off tests on coated reference (NT) and plasma-treated (PTA, PTB) MDF specimens as prepared and those exposed to AAW.

Figure 5 shows weight differences after 3 days of water immersion for coated reference (NT) and plasma-treated (PTA-PTE) specimens. Regarding MDF, the water uptake is reduced by 6 % for plasma pre-treatment PTB and by 15 % for plasma pre-treatment PTA.

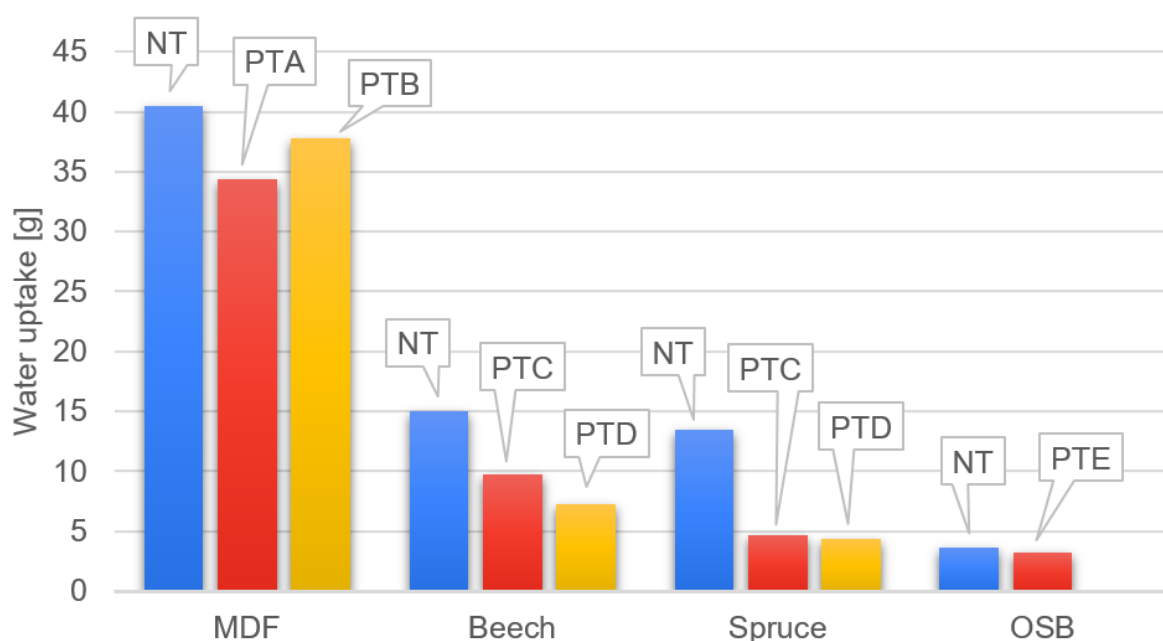


Figure 5: Weight differences after 3 days of water immersion for coated reference (NT) and plasma-treated (PTA, PTB, PTC, PTD, PTE) specimens of all substrates (MDF, beech, spruce, and OSB).

3.2 Performance of coated spruce samples

The total colour change ΔE during the AAW is less pronounced on coated spruce, if a plasma pre-treatment was carried out prior to the coating application. The colour changes in the L^* parameter is notably higher on the reference sample, whereas the changes in a^* and b^* values are slightly higher on the sample that was pre-treated according to protocol plasma treatment C (PTC) as given in section 2.2.2. The detailed values are summarized in Table 5.

Table 5: Change of CIELAB colour parameters with increasing AAW time on plasma pre-treated (PTC) and non-treated (NT) coated spruce samples.

Weathering Time / h	NT				PTC			
	ΔE	ΔL^*	Δa^*	Δb^*	ΔE	ΔL^*	Δa^*	Δb^*
10	1.55	-1.65	-0.51	-1.16	1.28	-1.01	-0.99	-1.69
50	1.81	-1.88	-0.43	-1.50	1.69	-1.38	-1.25	-2.16
63	2.07	-2.19	-0.72	-1.70	1.66	-1.44	-1.25	-1.95

Figure 6 depicts the development of the gloss values under 20°, 60° and 85° incident light angle for both, the plasma pre-treated and the non-treated reference samples. The initial values before weathering reveal a higher gloss value on the plasma pre-treated samples by a factor of 2.2, 2.3 and 1.5 at 20°, 60° and 85°, respectively. These ratios stay at similar values during the entire aging time. For both, reference and plasma pre-treated samples, the absolute gloss values at 20° and 60° slightly increase during weathering, whereas the values at 85° slightly decrease. The detailed values are summarized in Table S2 (Dahle et al. 2020).

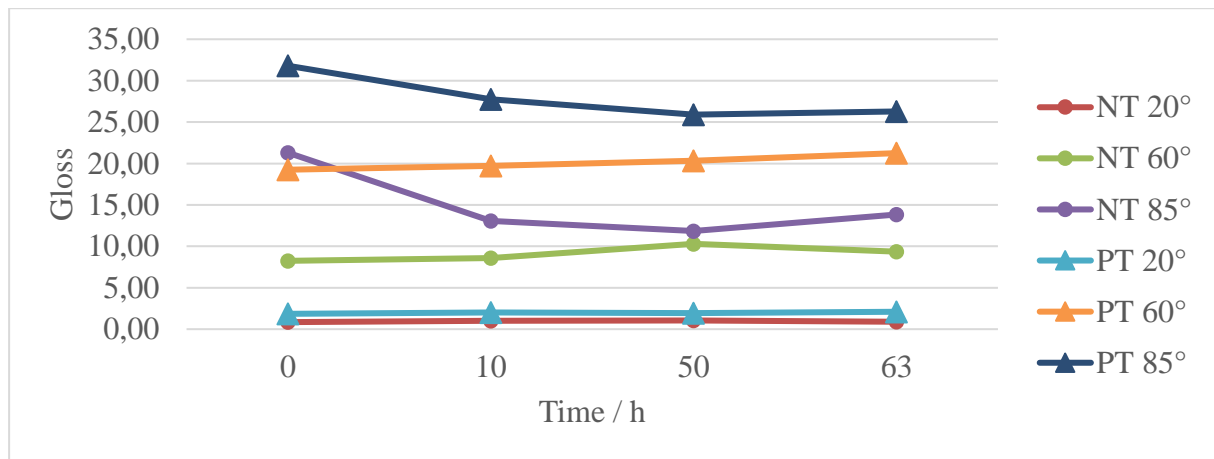


Figure 6: Change of gloss value under 20°, 60° and 85° over AAW time on plasma pre-treated (PTC) and non-treated (NT) coated spruce samples.

Figure 7 displays CLSM images of a non-treated, coated spruce specimen after 63 h AAW at 20× magnification (left image, $643 \times 644 \mu\text{m}^2$) with a vertical range of $\Delta Z = 82 \mu\text{m}$ as well as at 50× magnification (right image, $256 \times 257 \mu\text{m}^2$) with a vertical range of $\Delta Z = 57 \mu\text{m}$.

In comparison, Figure 8 exhibits CLSM images of a plasma pre-treated (PTC), coated spruce specimen after 63 h AAW at 20× magnification (left image, $643 \times 644 \mu\text{m}^2$) with a vertical range of $\Delta Z = 137 \mu\text{m}$ as well as at 50× magnification (right image, $256 \times 257 \mu\text{m}^2$) with a vertical range of $\Delta Z = 82 \mu\text{m}$.

The morphology of the surfaces is comparable, both showing round structures representing holes and particles, which are slightly larger but less densely distributed on the PT surfaces. This is reflected by roughness values of $Sq = 6.8 \mu\text{m}$ and $Sq = 3.2 \mu\text{m}$ at 20× and 50× magnification, respectively, for the PT specimen as compared to $Sq = 2.3 \mu\text{m}$ and $Sq = 1.2 \mu\text{m}$ for the non-treated specimen.

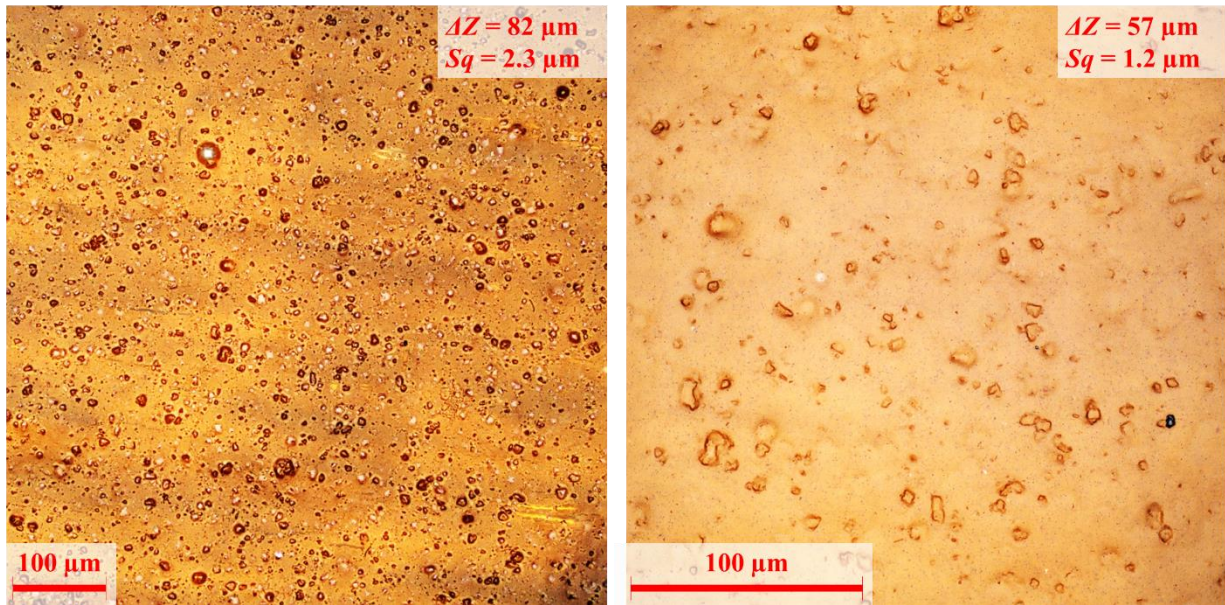


Figure 7: CLSM images of the coated spruce reference sample after 63 h of weathering at 20× (left) and 50× magnification (right).

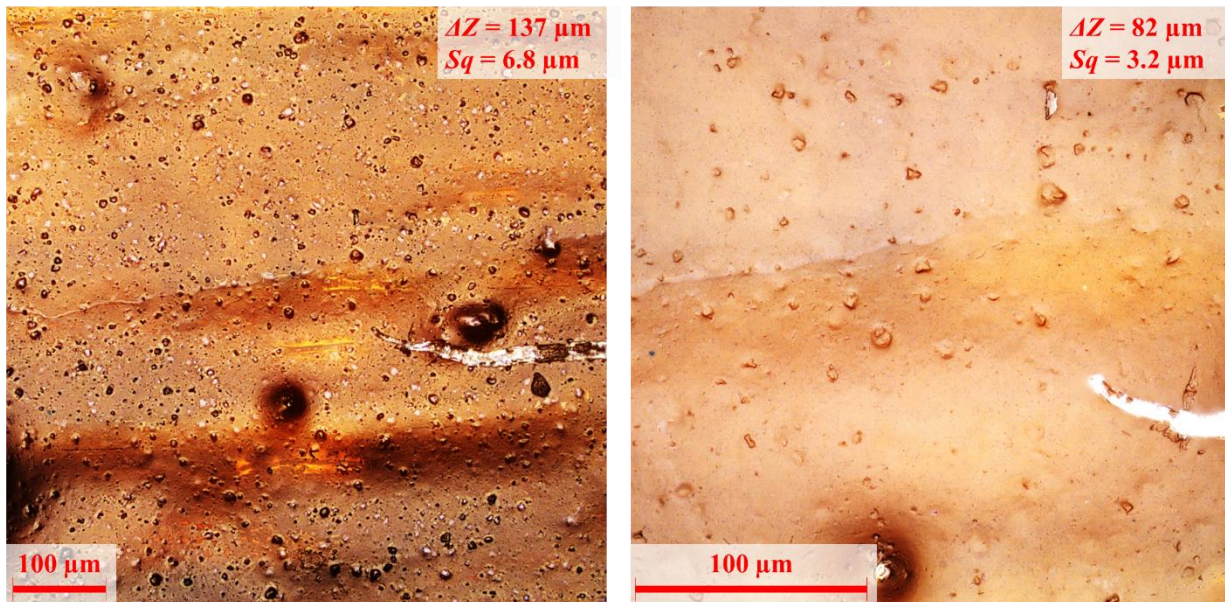


Figure 8: CLSM images of the plasma pre-treated (PTC), coated spruce sample after 63 h of weathering at 20× (left) and 50× magnification (right).

Figure 9 shows the results for adhesion strengths and the corresponding standard deviations from series of pull-off tests on both, the coated spruce reference specimens (NT) and the spruce specimens treated according to protocols plasma treatment C (PTC) and plasma treatment D (PTD) prior to coating application as described in section 2.2.2. The tests were carried out both, on as-prepared samples and on samples after 63 h of AAW. As-prepared NT and PTC specimen yielded comparable adhesive bond strengths slightly below 4 MPa, but with considerably less variations on the plasma-treated specimen as indicated by a standard deviation of only about 1/3rd of the reference specimen. The PTD specimen, however, exhibited even higher variations and a bond strength just slightly above 3 MPa. After weathering, the bond strength was reduced to 3.4 MPa on the NT specimen, whereas it remained at 4.1 MPa for the PTC specimen with even lower variations than before. In all cases, a cohesive failure inside the substrate did take place, the

fracture line being consistently deeper inside the plasma pre-treated substrates than for the reference specimens.

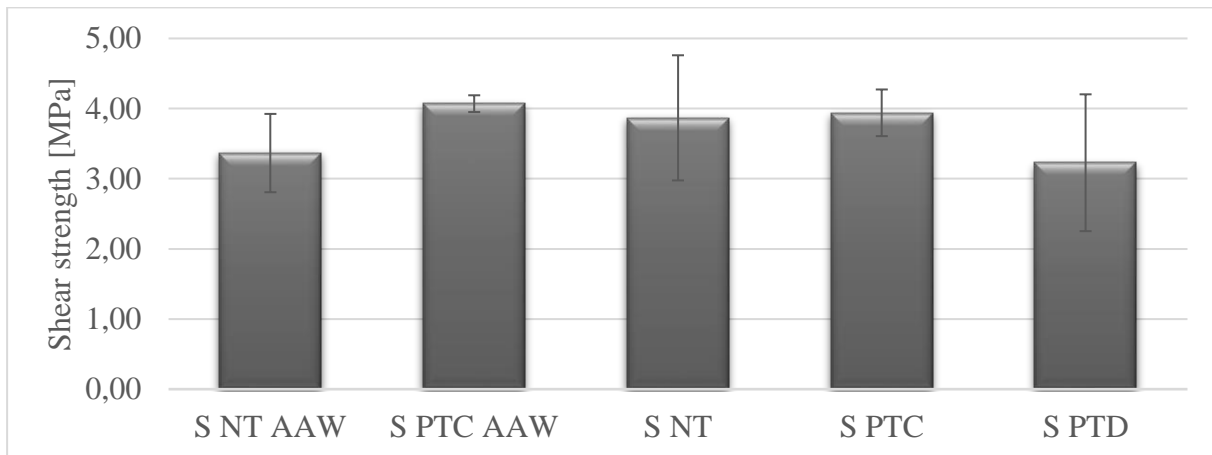


Figure 9: Adhesion strengths and corresponding standard deviations from pull-off tests on coated reference (NT) and plasma-treated (PTC, PTD) spruce specimens as prepared and AAW.

In Figure 5, weight differences after 3 days of water immersion for coated reference (NT) and plasma-treated (PTA-PTE) specimens are shown. Regarding beech, the water uptake is reduced by 35 % for plasma pre-treatment PTC and by 51 % for plasma pre-treatment PTD.

3.3 Performance of coated beech samples

The total colour change during the AAW is much stronger pronounced on the coated sample, that was pre-treated according to protocol plasma treatment C (PTC, c.f. section 2.2.2) prior to the coating application. This behaviour strongly differs from all other investigated samples. The detailed values are summarized in Table 6.

Table 6: Change of CIELAB colour parameters with increasing AAW time on plasma pre-treated (PTC) and non-treated (NT) coated beech samples.

Weathering time [h]	NT				PTC			
	ΔE	ΔL^*	Δa^*	Δb^*	ΔE	ΔL^*	Δa^*	Δb^*
10								
50								
63								

Figure 10 exhibits the development of the gloss values under 20°, 60° and 85° incident light angle for both, the plasma pre-treated and the non-treated reference samples. The absolute values at 20°, 60° and 85° are comparable and within their margins of error for both samples throughout the weathering. At 85° incident angle, the gloss values notably decrease within the first 10 hours. At 20° and 60°, gloss values remain the same throughout the weathering. The detailed values are summarized in Table S3 (Dahle et al. 2020).

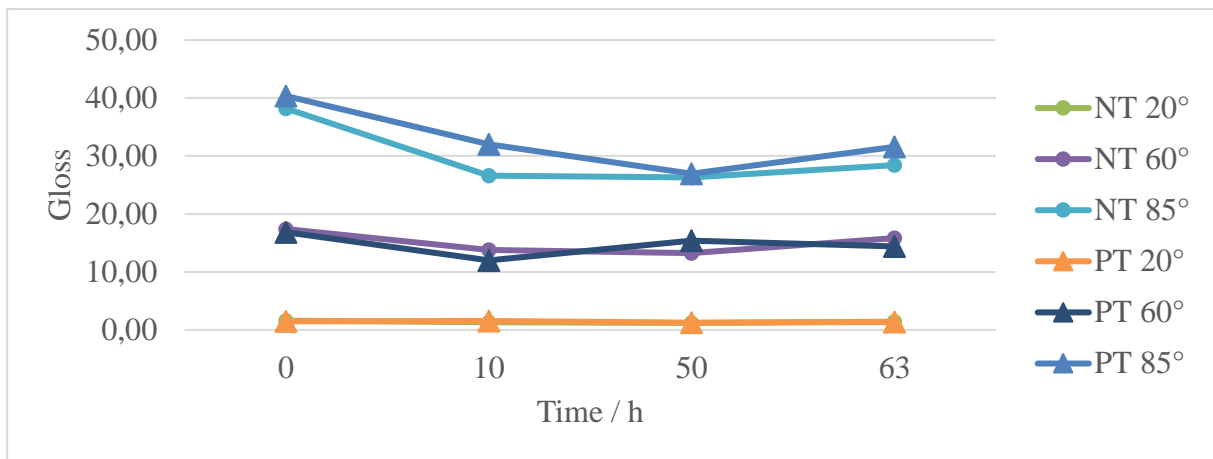


Figure 10: Change of gloss value under 20°, 60° and 85° over AAW time on plasma pre-treated (PTC) and non-treated (NT) coated beech samples.

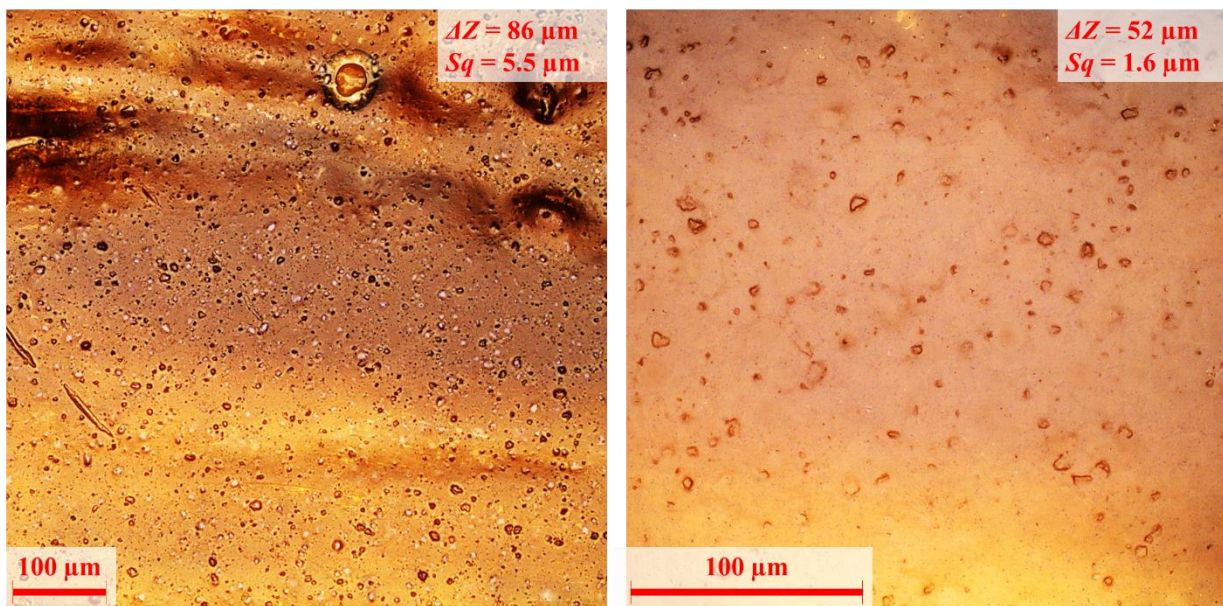


Figure 11 shows CLSM images of a non-treated, coated beech specimen after 63 h AAW at 20× magnification (left image, $643 \times 644 \mu\text{m}^2$) with a vertical range of $\Delta Z = 86 \mu\text{m}$ as well as at 50× magnification (right image, $256 \times 257 \mu\text{m}^2$) with a vertical range of $\Delta Z = 52 \mu\text{m}$.

In comparison, Figure 12 displays CLSM images of a plasma pre-treated (PTC), coated beech specimen after 63 h AAW at 20× magnification (left image, $643 \times 644 \mu\text{m}^2$) with a vertical range of $\Delta Z = 120 \mu\text{m}$ as well as at 50× magnification (right image, $256 \times 257 \mu\text{m}^2$) with a vertical range of $\Delta Z = 76 \mu\text{m}$.

All samples exhibited small (diameter $\sim 10 \mu\text{m}$) particles and holes regularly distributed across their surfaces. The roughness values are comparable for NT and PTC samples, as well, with values of $5.5 \mu\text{m}$ and $6.4 \mu\text{m}$ at 20× and $1.6 \mu\text{m}$ and $3.8 \mu\text{m}$ at 50× magnification, respectively.

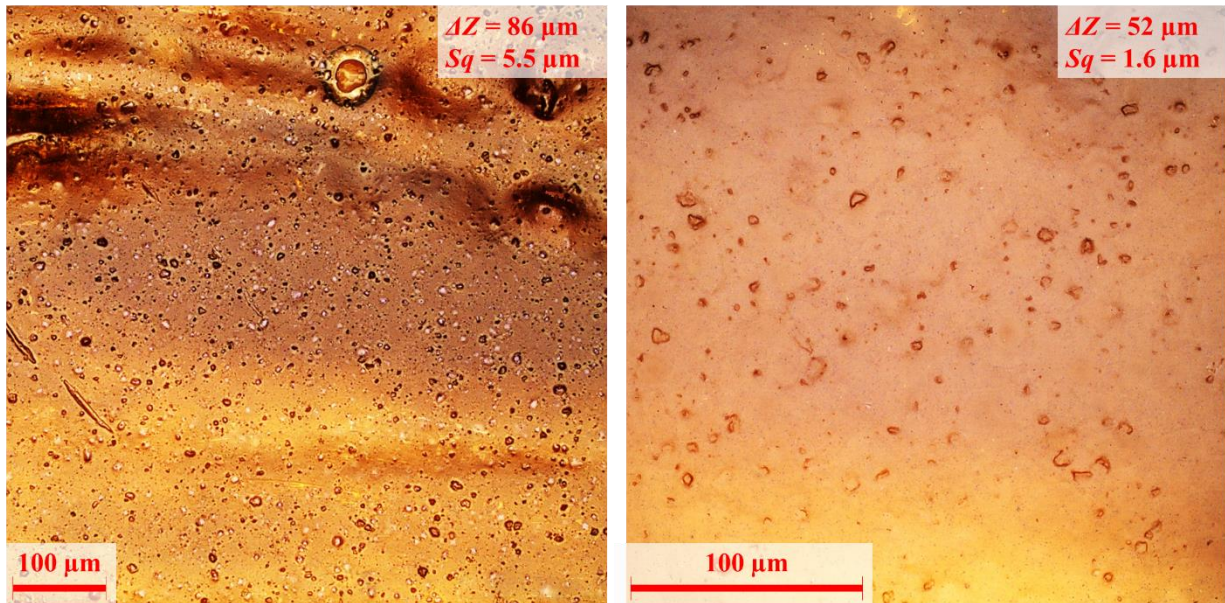


Figure 11: CLSM images of the coated beech reference sample after 63 h of weathering at 20× (left) and 50× magnification (right).

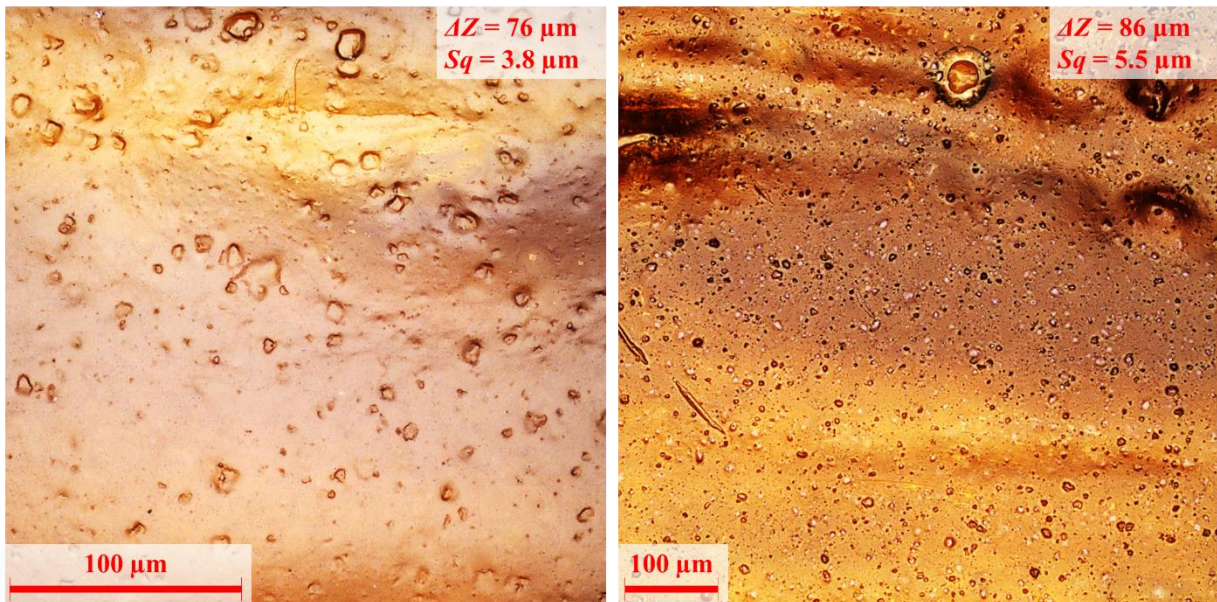


Figure 12: CLSM images of the plasma pre-treated (PTC), coated beech sample after 63 h of weathering at 20× (left) and 50× magnification (right).

Figure 13 exhibits shows the results for adhesion strengths and the corresponding standard deviations from series of pull-off tests on both, the coated beech reference specimens (NT) and the beech specimens treated according to protocols plasma treatment C (PTC) and plasma treatment D (PTD) prior to coating application as described in section 2.2.2. The tests were carried out both, on as-prepared samples and on samples after 63 h of AAW. Before weathering, adhesion strengths between 7 MPa and 8 MPa were determined, with slightly higher values for the non-treated specimen as compared to both of the plasma pre-treated samples. After 63 h of AAW, however, bond strengths were reduced to approx. 2 MPa, with a marginally higher value on the plasma pre-treated (PTC) sample. The as-prepared samples exhibited a cohesive failure inside the substrate for both, plasma pre-treated and reference specimens. The specimens after 63 h of AAW, however, all reproducibly yielded a cohesive failure at the surface of the test dolly.

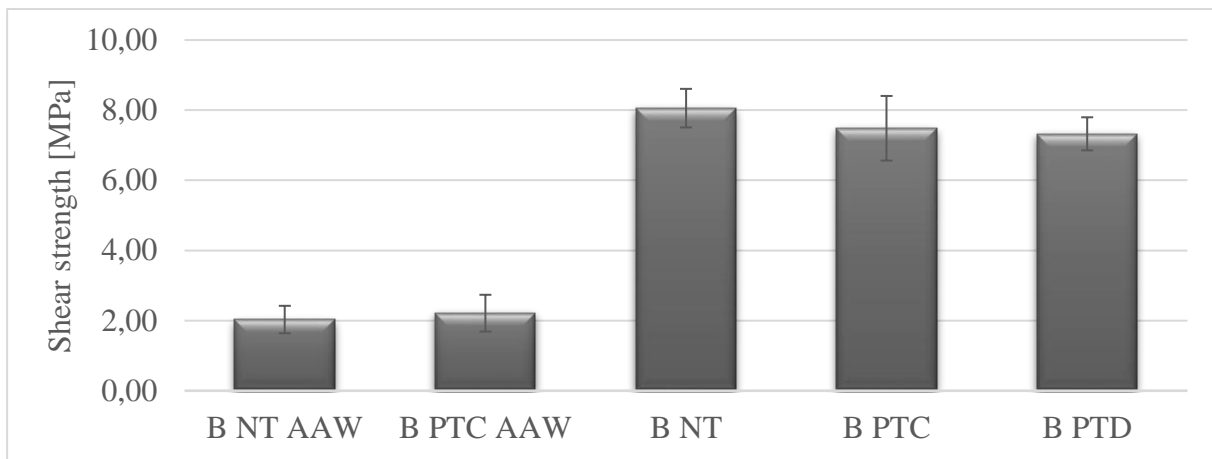


Figure 13: Adhesion strengths and corresponding standard deviations from pull-off tests on coated reference (NT) and plasma-treated (PTC, PTD) beech specimens as prepared and AAW.

In Figure 5, weight differences after 3 days of water immersion for coated reference (NT) and plasma-treated (PTA-PTE) specimens are shown. Regarding spruce, the water uptake is reduced by 65 % for plasma pre-treatment PTC and by 68 % for plasma pre-treatment PTD.

3.4 Performance of coated OSB samples

The total colour change during the AAW is much stronger pronounced on the coated reference sample as compared to the sample that was treated according to protocol plasma treatment E (PTE) prior to the coating application, as described in section 2.2.3. The detailed values are summarized in Table 7.

Table 7: Change of CIELAB colour parameters with increasing AAW time on plasma pre-treated (PTE) and non-treated (NT) coated OSB samples.

Weathering Time / h	NT				PTE			
	ΔE	ΔL^*	Δa^*	Δb^*	ΔE	ΔL^*	Δa^*	Δb^*
10	1.11	0.22	-0.02	0.24	0.37	-0.29	-0.29	-0.24
50	0.52	-0.33	-0.26	-0.30	0.52	-0.30	-0.41	-0.60
63	0.84	-0.66	-0.49	-0.92	0.53	-0.40	-0.29	-0.40

Figure 14 depicts the development of the gloss values under 20°, 60° and 85° incident light angle for both, the plasma pre-treated and the non-treated reference samples. The absolute values are within their margins of error for both samples and the values at 20° and 60° stay at the same values throughout the weathering. At 85° incident angle, the gloss values notably decrease during the whole weathering time. The detailed values are summarized in Table S4 (Dahle et al. 2020).

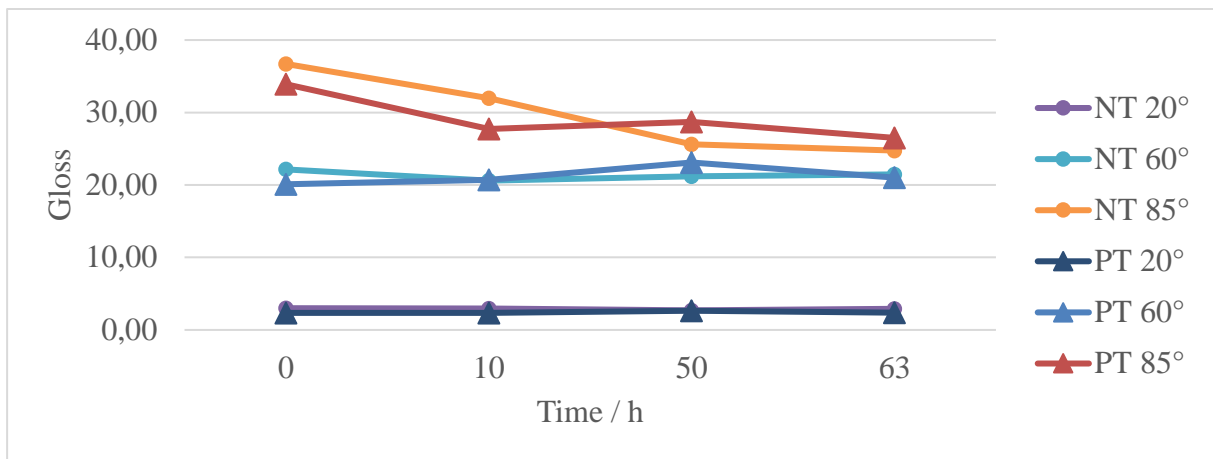


Figure 14: Change of gloss value under 20°, 60° and 85° over AAW time on plasma pre-treated (PTE) and non-treated (NT) coated OSB samples.

Figure 15 displays CLSM images of a non-treated, coated OSB specimen after 63 h AAW at 20× magnification (left image, $643 \times 644 \mu\text{m}^2$) with a vertical range of $\Delta Z = 42 \mu\text{m}$ as well as at 50× magnification (right image, $256 \times 257 \mu\text{m}^2$) with a vertical range of $\Delta Z = 8 \mu\text{m}$.

Figure 16 exhibits CLSM images of a plasma pre-treated (PTE), coated OSB specimen after 63 h AAW at 20× magnification (left image, $643 \times 644 \mu\text{m}^2$) with a vertical range of $\Delta Z = 80 \mu\text{m}$ as well as at 50× magnification (right image, $256 \times 257 \mu\text{m}^2$) with a vertical range of $\Delta Z = 67 \mu\text{m}$. The depicted images were taken on top of flat strands for better visualization of the representative morphology and appearance. At rough parts of the surfaces, i.e. in holes between the top layer of strands, the microstructure of the coatings' surfaces was largely comparable. The morphology of both, the NT and the PTE samples was comparable as represented by roughness values of $Sq = 2.9 \mu\text{m}$ and $Sq = 2.4 \mu\text{m}$ at 20× as well as $Sq = 0.6 \mu\text{m}$ and $Sq = 1.7 \mu\text{m}$ at 50× magnification, respectively.

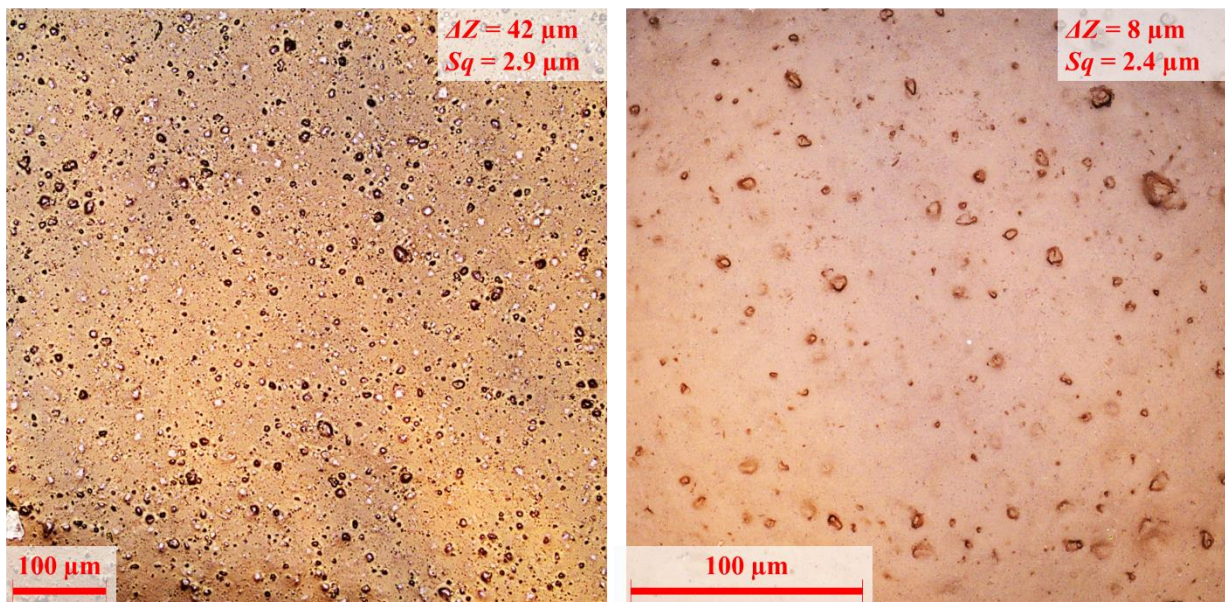


Figure 15: CLSM images of the coated OSB reference sample after 63 h of weathering at 20× (left) and 50× magnification (right).

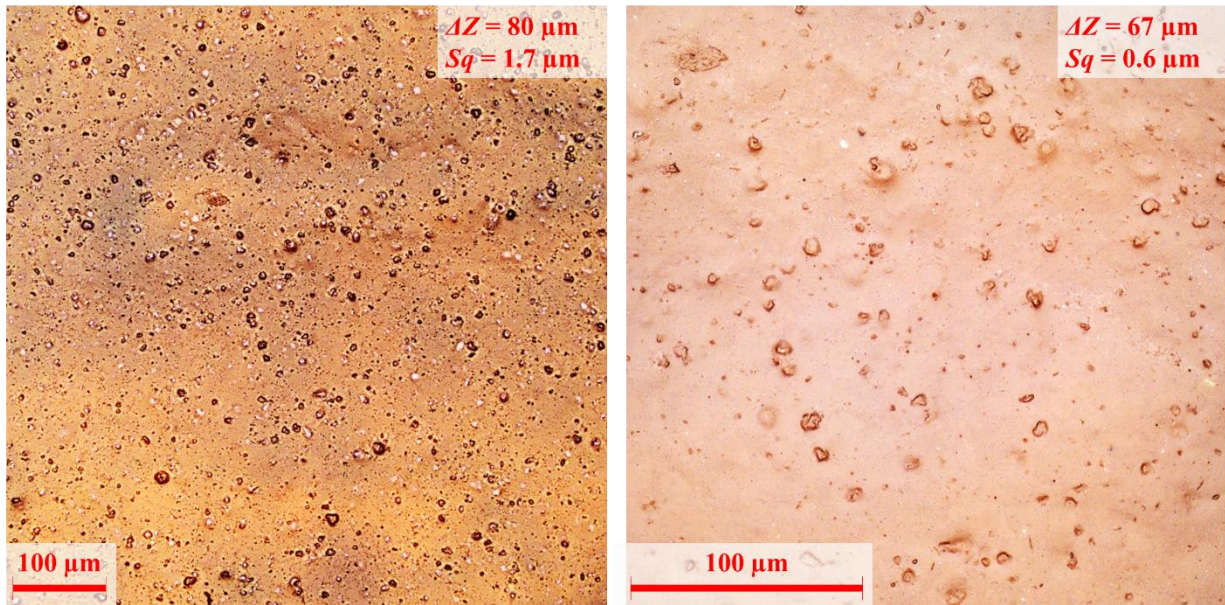


Figure 16: CLSM images of the plasma pre-treated (PTE), coated OSB sample after 63 h of weathering at 20× (left) and 50× magnification (right).

Figure 17 shows the results for adhesion strengths and the corresponding standard deviations from series of pull-off tests on both, the coated reference (NT) and the plasma-treated (PTE) OSB specimens. The tests were carried out both, on as-prepared samples and on samples after 63 h of AAW. Test dollies were placed on homogeneous surface areas and where possible on single strands to yield representative results. However, variations were comparatively large and therefore, almost all determined values for the adhesive bond strengths are within their large margins of error. Nevertheless, non-treated samples appear at adhesive bond strength largely around 2 MPa and thus at slightly lower values than the plasma pre-treated (PTE) OSB samples with bond strengths around 2.5 MPa. Again, all failures were exclusively of cohesive type inside the substrate, with just one outlier at one reference specimen after AAW.

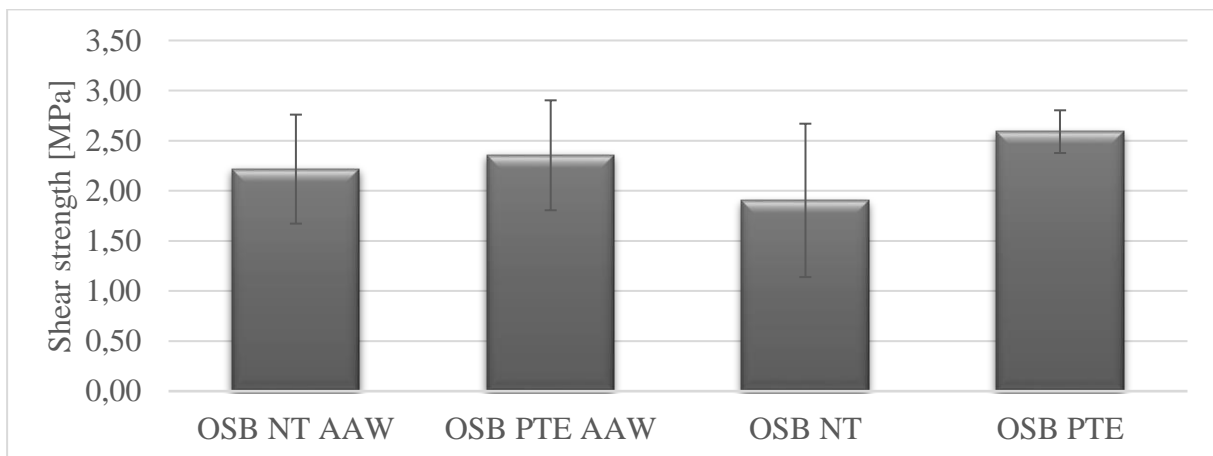


Figure 17: Adhesion strengths and corresponding standard deviations from pull-off tests on coated reference (NT) and plasma-treated (PTE) spruce specimens as prepared and AAW.

In Figure 5, weight differences after 3 days of water immersion for coated reference (NT) and plasma-treated (PTA-PTE) specimens are shown. Regarding OSB, the water uptake is reduced by 11 % for samples pre-treated according to plasma treatment procedure PTE.

4 CONCLUSIONS

The plasma pre-treatments did have an impact on the coating's performance on all substrates. The nature of the effect was quite different on the various substrates, though, regarding different aesthetical and mechanical aspects.

The colour changes are quite differently pronounced on the different substrates. On solid spruce, the plasma pre-treatments led to slightly lower colour changes during AAW in terms of ΔE and ΔL^* , whereas on solid beech, the same plasma pre-treatments caused an increased colour change during AAW for all ΔE , ΔL^* , Δa^* , and Δb^* . Both composite substrates OSB and MDF were in line with spruce, showing lower colour change during AAW for all ΔE , ΔL^* , Δa^* , and Δb^* on plasma pre-treated specimens, but with much lower differences between plasma pre-treated and reference samples.

The gloss parameters remained at approx. doubled values after AAW on the plasma pre-treated specimen as compared to the reference ones for solid spruce wood and for the MDF composite. On beech and OSB samples, however, the gloss values were equal for plasma pre-treated and reference specimens in all cases, i.e. before, during, and after the AAW.

The surface morphology was comparable on coated solid spruce and beech wood as well as on the coated OSB composite specimens. For coated MDF composites, however, the non-treated reference samples developed macroscopic valleys and ridges during the weathering. The AAW process led to swelling of all composite samples, particularly of the MDF specimens, due to their unprotected back and sides. However, the swelling of the non-treated MDF sample was stronger by 12.7 % as compared to the swelling of the plasma pre-treated sample, thus indicating a clear impact of the plasma pre-treatment on the coating's performance for moisture resistance.

The adhesion of the coating and the corresponding adhesion strengths before weathering were largely comparable between the non-treated samples and the corresponding plasma pre-treated samples, i.e. pairs of values fall well into each other's margin of error. Differences after the weathering were negligible on beech, but on spruce, the adhesion strength on the non-treated sample was reduced by 13 %, whereas the bond strength on the plasma pre-treated specimen remained at the initial value.

Due to particularly strong variations, apparent differences on coated OSB between plasma pre-treated and non-treated specimens are still well within the margins of error, so that no significant impact of the plasma treatment can be deduced, neither can it be excluded.

On MDF, no values could be obtained after weathering due to the degradation of the substrates' bulk material.

The water immersion tests revealed an extraordinary reduction of the water uptake of $\frac{2}{3}$ on spruce and $\frac{1}{2}$ on beech for a coating that already was optimized for outdoor applications. On OSB substrates, a paraffin coating applied by the manufacturer already provides good protection against water uptake; the plasma pre-treatment, however, still yields an improvement and might, thus, be an interesting alternative to paraffin impregnation. On MDF, all samples performed relatively poorly due to the bulk properties of the material. The plasma pre-treatments did again yield a notable improvement to the commercial coating, but a simple plasma activation did not improve the performance well enough to qualify an industrial application on this material. Rather, the results indicate the necessity of a barrier that might be applied as interlayer between substrate and commercial coating, e.g. in the form of plasma polymerization.

In summary, plasma treatments have different impacts on the performance of water-borne stains on various wooden and wood-based materials. The particular influence of a given plasma device on a specific sample, however, should be determined for all new cases.

5 ACKNOWLEDGEMENTS

The authors thankfully acknowledge the provision of the plasma equipment by Plasmatreat GmbH, Steinhagen, Germany.

The authors acknowledge the financial support from the Slovenian Research Agency (research programme funding no. P4-0015, “Wood and lignocellulose composites”).

This project has received funding from the European Union's Horizon 2020 research and innovation programme under grant agreement No. 745936.

6 REFERENCES

Altgen D, Bellmann M, Wascher R, Viöl W, Mai C (2015). Enhancing mechanical properties of particleboards using plasma treated wood particles. *Eur. J. Wood Prod.* **73**: 219-223.

Altgen D, Grigsby W, Altgen M, Rautkari L, Mai C (2019). Analyzing the UF resin distribution in particleboards by confocal laser microscopy. *Composites, Part A* **125**: 105529.

Baltazar-Y-Jimenez A, Bismarck A (2007). Surface modification of lignocellulosic fibres in atmospheric air pressure plasma. *Green Chemistry* **9**, 1057-1066.

Baltazar-Y-Jimenez A, Bistriz M, Schulz E, Bismarck A (2008). Atmospheric air pressure plasma treatment of lignocellulosic fibres: Impact on mechanical properties and adhesion to cellulose acetate butyrate. *Composites Science and Technology*, **68**(1), 215-227. DOI: 10.1016/j.compscitech.2007.04.028.

Bardak S, Sarı B, Nemli G, Kırıcı H, Baharoğlu M (2011). The effect of décor paper properties and adhesive type on some properties of particleboard. *Int. J. Adhes. Adhes.* **31**: 412-415.

Blanchard V, Blanchet P, Riedl B (2009). Surface energy modification by radiofrequency inductive and capacitive plasmas at low pressures in sugar maple: An exploratory study. *Wood and Fiber Science*, **41**(3), 245-254.

CIE (2001). Improvement to industrial colour-difference evaluation. Vienna: CIE Publication No. 142-2001, Central Bureau of the CIE.

Dahle S, Žigon J, Uranjek I, Petrič M (2020) Raw and analyzed data for manuscript: "Performance of a water-borne stain on beech, spruce, MDF and OSB improved by plasma pre-treatment". Zenodo, version 1.0.0. DOI: 10.5281/zenodo.3733833

Dam T N (2017). Environmental enhancing adhesion properties of Wood-Plastic Composites by plasma at atmospheric pressure. *2017 International Conference on System Science and Engineering (ICSSE)*, 652-655. ISBN: 978-1-5386-3422-6. DOI: 10.1109/ICSSE.2017.8030956.

De Cademartori P H G, Carvalho A R, Marangoni P R D, Berton M A C, Blanchet P, Muniz G I B, Magalhães W L E (2016). Adhesion performance and film formation of acrylic emulsion coating on medium density fiberboard treated with Ar plasma. *International Journal of Adhesion & Adhesives*, **70**, 322-328.

De Vetter L, Van den Bulcke J, Van Acker J (2011). Envelope treatment of wood based materials with concentrated organosilicons. *European Journal of Wood and Wood Products*, **69**, 397–406. DOI: 10.1007/s00107-010-0448-4

Durmaz S, Özgenç Ç, Avcı E, Boyacı İ H (2020). Weathering performance of waterborne acrylic coating systems on flat-pressed wood–plastic composites. *Journal of Applied Polymer Science*, **137**, 48518. DOI: 10.1002/app.48518

EN ISO 927-5 (2007) Paints and varnishes - Coating materials and coating systems for exterior wood - Part 5: Assessment of the liquid water permeability. European Committee for Standardization, Brussels, Belgium.

EN ISO 2813 (1997). Paints and varnishes - Determination of specular gloss of non-metallic paint films at 20°, 60° and 85°. European Committee for Standardization, Brussels, Belgium.

EN ISO 4246 (2016) Paints and varnishes - Pull-off test for adhesion. European Committee for Standardization, Brussels, Belgium.

EN ISO 11341 (2004) Paints and varnishes - Artificial weathering and exposure to artificial radiation - Exposure to filtered xenon-arc radiation. European Committee for Standardization, Brussels, Belgium.

Haase J G, Leung L H, Evans P D (2019). Plasma pre-treatments to improve the weather resistance of polyurethane coatings on black spruce wood. *Coatings*, **9**(1), 8.

Hämäläinen K, Kärki T (2013). Effects of Atmospheric Plasma Treatment on the Surface Properties of Wood-Plastic Composites. *Advanced Materials Research*, 718-720, 176-185. DOI: 10.4028/www.scientific.net/AMR.718-720.176

Istek A, Aydemir D, Aksu S (2010). The effect of décor paper and resin type on the physical, mechanical, and surface quality properties of particleboards coated with impregnated décor papers. *BioResources*, **5**(2), 1074-1083.

Jamali A, Evans P D (2011). Etching of wood surfaces by glow discharge plasma. *Wood Science and Technology*, **45**, 169-182.

Jordá-Vilaplana A, Sánchez-Nácher L, Fombuena V, García-García D, Carbonell-Verdú A (2015). Improvement of mechanical properties of polylactic acid adhesion joints with bio-based adhesives by using air atmospheric plasma treatment. *Journal of Applied Polymer Science*, **132**, 42391. DOI: 10.1002/app.42391

Keskin H, Tekin A (2011). Abrasion resistances of cellulosic, synthetic, polyurethane, waterborne and acidhardening varnishes used woods. *Constr. Build. Mater.*, **25**: 638-643.

Kiguchi M, Kataoka Y, Matsunaga H, Yamamoto K, Evans P D (2007). Surface deterioration of wood-flour polypropylene composites by weathering trials. *Journal of Wood Science*, **53**, 234–238. DOI: 10.1007/s10086-006-0838-8.

Kraus E, Baudrit B, Kretschmer K, Heidemeyer P, Bastian M (2015). Wie sind beste Langzeiteigenschaften erreichbar? - Geklebte Holz-Kunststoff-Verbunde im Ausseneinsatz. *adhäsion KLEBEN & DICHTEN*, **59**(1-2), 42-47.

LIGNA (2013). Holz und Klebstoff - eine natürliche Verbindung. *adhäsion KLEBEN & DICHTEN*, **57**(4), 22-25.

Liston E M, Martinu L, Wertheimer M R (1993). Plasma surface modification of polymers for improved adhesion: a critical review. *J. Adhes. Sci. Technol.*, **7**(10): 1091-1127.

Lütke-meier B, Konnerth J, Militz H (2016) Bonding performance of modified wood. Distinctive influence of plasma pre-treatments on bonding strength. *World Conference on Timber Engineering 2016 e-book*, 518-527.

Melamies I A (2014). Feeling the rush of speed - New impregnation process for race skis. *JOT International Surface Technology*, **3.2014**, 32-35.

Nejad M, Shafaghi R, Pershin L, Mostaghimi J, Cooper P (2017). Thermal Spray Coating: A New Way of Protecting Wood. *BioResources*, **12**(1), 143.

Nemli G, Hiziroglu S (2009). Effect of press parameters on scratch and abrasion resistance of overlaid particleboard panels. *J. Compos. Mater.*, **43**, 13: 1413-1420.

Perisse F, Menecier S, Duffour E, Vacher D, Monier G, Destrebecq J-F, Czarniak P, Górski J, Wilkowski J (2017). MDF treatment with a Dielectric Barrier Discharge (DBD) torch. *Int. J. Adhes. Adhes.* **79**, 18-22.

Podgorski L, Roux M (1999). Wood modification to improve the durability of coatings. *Surf. Coat Int.*, **82**, 590-596.

Reinprecht L, Tiño R, Šomšák M (2018). Adhesion of coatings to plasma modified wood at accelerated weathering. In: *European Conference on Wood Modification 2018 (ECWM9)*, Arnhem, The Netherlands (On-line Proceedings). Ed. Creemers J, Houben T, Tjeerdsma B, Militz H, Junge B, Gootjes J. 205-209.

Riedl B, Angel C, Prigent J, Blanchet P, Stafford L (2014). Effect of wood surface modification by atmospheric-pressure plasma on waterborne coating adhesion. *BioRes.*, **9**(3), 4908-4923.

Rolleri A, Roffael E (2010). Influence of the surface roughness of particleboards and their performance towards coating. *Maderas ciencia y tecnologia*, **12**(2): 143-148.

Sharma G, Wu W, Dalal E N (2005). The CIEDE2000 color-difference formula: Implementation notes, supplementary test data, and mathematical observations. *Color Research & Applications*, **30**(1), 21-30. doi:10.1002/col.20070.

Sharma G, Wu W, Dalal E N. Supplemental test data and excel and matlab implementations of the CIEDE2000 color difference formular. Downloaded from <http://www.ece.rochester.edu/~gsharma/ciede2000/> on 21.02.2020.

Straccia A, Haack A P, Holubka J W, Murray T (2008) Method for decorating a plastic component with a coating. US Patent application US2008/0138532-A1.

- Veigel S, Grüll G, Pinkl S, Obersriebnig M, Müller U, Gindl-Altmutter W (2014). Improving the mechanical resistance of waterborne wood coatings by adding cellulose nanofibers. *React. Funct. Polym.*, **85**, 214-220.
- Wascher R, Avramidis G, Vetter U, Damm R, Peters F, Militz M, Viöl W (2014). Plasma induced effects within the bulk material of wood veneers. *Surface & Coatings Technology*, **259**, 62-67.
- Wascher R, Kühn C, Avramidis G, Bicke S, Militz H, Ohms G, Viöl W (2017). Plywood made from plasma-treated veneers: melamine uptake, dimensional stability, and mechanical properties. *Journal of Wood Science*, **63**, 338-349.
- Wolf R, Sparavigna A C (2010). Role of plasma surface treatments on wetting and adhesion. *Engineering* **2**: 397-402.
- Wolkenhauer A, Militz H, Viöl W (2008). Increased PVA-glue adhesion on particle board and fibre board by plasma treatment. *Holz Roh- Werkst.*, **66**, 143-145.
- Wolkenhauer A, Avramidis G, Hauswald E, Loose S, Viöl W, Militz H (2009). Investigations on the drying behaviour of adhesives on plasma-treated wood materials. *Wood Res.*, **54**(1): 59-66.
- Žigon J, Petrič M, Dahle S (2018). Dielectric barrier discharge (DBD) plasma pretreatment of lignocellulosic materials in air at atmospheric pressure for their improved wettability: a literature review. *Holzforschung*, **72**(11): 979-991.
- Žigon J, Dahle S (2019). Improvement of plasma treatment efficiency of wood and coating process by sodium chloride aqueous solutions. *Proligno*, **15**(4), 260-267.
- Žigon J, Petrič M, Dahle S (2019). Artificially aged spruce and beech wood surfaces reactivated using FE-DBD atmospheric plasma. *Holzforschung*, **73**(12), 1069-1081.